

Multiwavelength Milky Way

“Multiwavelength Milky Way”

<http://adc.gsfc.nasa.gov/mw/milkyway.html> による

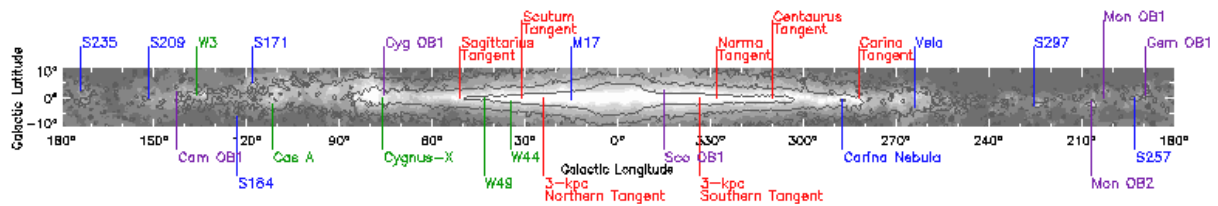


図 1 Major structural features of the Milky Way (red), optical H II regions (blue), radio sources (green), and OB associations (purple) are labeled in the finder chart. The image in the finder chart is derived from the IRAS 100 micron map of intensity with contours from the COBE DIRBE 3.5 micron map overlaid.



1 Radio Continuum (408 MHz)

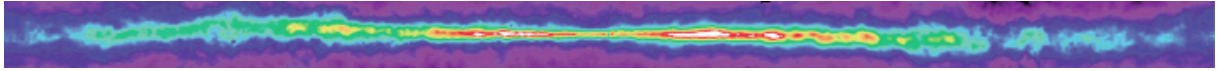


図 2 Radio 0.4 GHz

Intensity of radio continuum emission from high-energy charged particles in the Milky Way, from surveys with ground-based radio telescopes (Jodrell Bank Mark I and Mark IA, Bonn 100-meter, and Parkes 64-meter). At this frequency, most of the emission is from electrons moving through the interstellar magnetic field at nearly the speed of light. Shock waves from supernova explosions accelerate electrons to such high speeds, producing especially intense radiation near these sources. Emission from the supernova remnant Cas A near 110° longitude is so intense that the diffraction pattern of the support legs for the radio receiver on the telescope is visible as a cross shape.

$$408 \text{ MHz} = 0.734785 \text{ m} = 734 \text{ mm}$$

2 Atomic Hydrogen

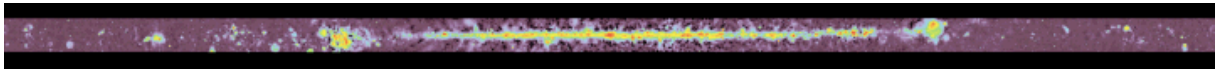


☒ 3 Atomic Hydrogen

Column density of atomic hydrogen, derived on the assumption of optically thin emission, from radio surveys of the 21-cm transition of hydrogen. The 21-cm emission traces the "cold and warm" interstellar medium, which on a large scale is organized into diffuse clouds of gas and dust that have sizes of up to hundreds of light-years. Most of the image is based on the Leiden-Dwingeloo Survey of Galactic Neutral Hydrogen using the Dwingeloo 25-m radio telescope; the data were corrected for sidelobe contamination in collaboration with the University of Bonn.

$$1.4 \text{ GHz} = 0.214137 \text{ m} = 214 \text{ mm}$$

3 Radio Continuum (2.4-2.7 GHz)



☒ 4 Radio 2.7 GHz

Intensity of radio continuum emission from hot, ionized gas and high-energy electrons in the Milky Way, from surveys with both the Bonn 100-meter, and Parkes 64-meter radio telescopes. Unlike most other views of our Galaxy presented here, these data extend to latitudes of only 5° from the Galactic plane. The majority of the bright emission seen in the image is from hot, ionized regions, or is produced by energetic electrons moving in magnetic fields. The higher resolution of this image, relative to the 408 MHz picture above, shows Galactic objects in more detail. Note that the bright "ridge" of Galactic radio emission, appearing prominently in the 408 MHz image, has been subtracted here in order to show Galactic features and objects more clearly.

$$2.4 \sim 2.7 \text{ GHz} = 0.111034 \sim 0.124914 \text{ GHz} = 111 \sim 125 \text{ mm}$$

4 Molecular Hydrogen

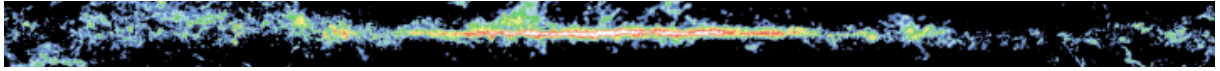


图 5 Molecular Hydrogen

Column density of molecular hydrogen inferred from the intensity of the $J = 1-0$ spectral line of carbon monoxide, a standard tracer of the cold, dense parts of the interstellar medium. Such gas is concentrated in the spiral arms in discrete "molecular clouds." Most molecular clouds are sites of star formation. The molecular gas is pre-dominantly H_2 , but H_2 is difficult to detect directly at interstellar conditions and CO, the second most abundant molecule, is observed as a surrogate. The column densities were derived on the assumption of a constant proportionality between the column density of H_2 and the intensity of the CO emission.

$$115 \text{ GHz} = 0.00260689 \text{ m} = 2.6 \text{ mm}$$

5 Infrared

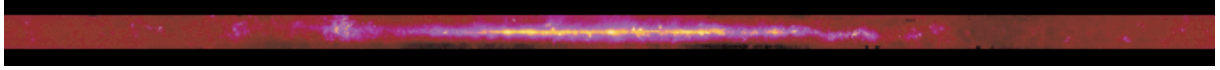


图 6 Infrared

Composite mid-and far-infrared intensity observed by the Infrared Astronomical Satellite (IRAS) in 12, 60, and 100 micron wavelength bands. The images are encoded in the blue, green, and red color ranges, respectively. Most of the emission is thermal, from interstellar dust warmed by absorbed starlight, including star-forming regions embedded in interstellar clouds. The display here is a mosaic of IRAS Sky Survey Atlas images. Emission from interplanetary dust in the solar system, the "zodiacal emission," was modeled and subtracted in the production of the Atlas.

$$3.0 \times 10^3 \sim 25 \times 10^3 \text{ GHz} = 0.0000119917 \sim 0.0000999308 \text{ m} = 12 \sim 100 \mu\text{m}$$

6 Mid-infrared (6.8 -10.8 microns)



☒ 7 Mid Infrared

Mid-infrared emission observed by the SPIRIT III instrument on the Midcourse Space Experiment (MSX) satellite. Most of the diffuse emission in this wavelength band is believed to come from complex molecules called polycyclic aromatic hydrocarbons, which are commonly found both in coal and interstellar gas clouds. Red giant stars, planetary nebulae, and massive stars so young that they remain deeply embedded in their parental molecular gas clouds produce the multitude of small bright spots seen here. Unlike most of the other maps, this map extends only to 5° above and below the Galactic plane.

$$3.0 \times 10^3 \sim 25 \times 10^3 \text{ GHz} = 0.0000119917 \sim 0.0000999308 \text{ m} = 12 \sim 100 \mu\text{m}$$

7 Near Infrared



☒ 8 Near Infrared

Composite near-infrared intensity observed by the Diffuse Infrared Background Experiment (DIRBE) instrument on the Cosmic Background Explorer (COBE) in the 1.25, 2.2, and 3.5 micron wavelength bands. The images are encoded in the blue, green, and red color ranges, respectively. Most of the emission at these wavelengths is from relatively cool giant K stars in the disk and bulge of the Milky Way. Interstellar dust does not strongly obscure emission at these wavelengths; the maps trace emission all the way through the Galaxy, although absorption in the 1.25 micron band is evident toward the Galactic center region.

$$86 \times 10^3 \sim 240 \times 10^3 \text{ GHz} = 1.24914 \sim 3.48596 \mu\text{m}$$

8 | Optical



☒ 9 Optical

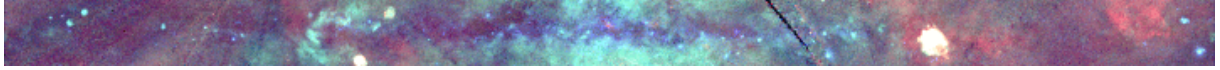
Intensity of visible (0.4 - 0.6 micron) light from a photographic survey. Due to the strong obscuring effect of interstellar dust, the light is primarily from stars within a few thousand light-years of the Sun, nearby on the scale of the Milky Way. The widespread bright red regions are produced by glowing, low-density gas. Dark patches are due to absorbing clouds of gas and dust, which are evident in the Molecular hydrogen and Infrared maps as emission regions. Stars differ from one another in color, as well as mass, size and luminosity. Interstellar dust scatters blue light preferentially, reddening the starlight somewhat relative to its true color and producing a diffuse bluish glow. This scattering, as well as absorption of some of the light by dust, also leaves the light diminished in brightness. The panorama was assembled from sixteen wide-angle photographs taken by Dr. Axel Mellinger using a standard 35-mm camera and color negative film. The exposures were made between July 1997 and January 1999 at sites in the United States, South Africa, and Germany. The image processing and mosaicing procedures are described in the document cited below. Image courtesy of A. Mellinger.

$$460 \times 10^3 \text{ GHz} = 6.517227 \times 10^{-7} \text{ m} = 6517 \text{ \AA}$$

9 | Ultraviolet

You might notice that missing from the list of images is the ultraviolet region of the electromagnetic (EM) spectrum. Ultraviolet radiation begins just past the blue/violet region of the visible (optical) spectrum, and ends when X-rays take over. The boundaries between named regions can get a little blurred, especially if the broad-band regions (example: infrared) are further broken into sub-regions (example: near infrared and far infrared). One reference on EM waves says microwaves extend from about 1 millimeter to about 10 centimeters. In that case, the map of molecular hydrogen would fall into the category of microwaves.

10 X-Ray

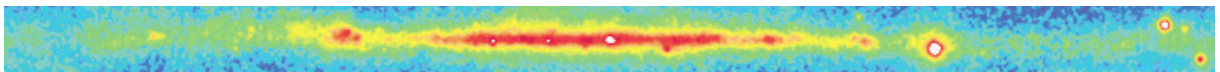


☒ 10 X-Ray

Composite X-ray intensity observed by the Position-Sensitive Proportional Counter (PSPC) instrument on the Röntgen Satellite (ROSAT). Images in three broad, soft X-ray bands centered at 0.25 , 0.75, and 1.5 keV are encoded in the red, green, and blue color ranges, respectively. In the Milky Way, extended soft X-ray emission is detected from hot, shocked gas. At the lower energies especially, the interstellar medium strongly absorbs X-rays, and cold clouds of interstellar gas are seen as shadows against background X-ray emission. Color variations indicate variations of absorption or of the temperatures of the emitting regions. The black regions indicate gaps in the ROSAT survey.

$$60 \sim 360 \times 10^6 \text{ GHz} = 8.32757 \times 10^{-10} \sim 4.99654 \times 10^{-9} \text{ m} = 8.32757 \sim 49.9654 \text{ \AA}$$

11 Gamma Ray



☒ 11 Gamma-Ray

Intensity of high-energy gamma-ray emission observed by the Energetic Gamma-Ray Experiment Telescope (EGRET) instrument on the Compton Gamma-Ray Observatory (CGRO). The image includes all photons with energies greater than 300 MeV. At these extreme energies, most of the celestial gamma rays originate in collisions of cosmic rays with hydrogen nuclei in interstellar clouds. The bright, compact sources near Galactic longitudes 185 ° , 195 ° , and 265 ° indicate high-energy phenomena associated with the Crab, Geminga, and Vela pulsars, respectively.

$$\nu > 2.4 \times 10^{13} \text{ GHz}, \quad \lambda < 1.24914 \times 10^{-14} \text{ m} = 1.24914 \times 10^{-4} \text{ \AA}$$